

**Interaction of slow  $N_2^+$  ions with the Si(001) surface: A combined photoemission and LEED study**

D. H. Baek

*Physics Department, Pohang Institute of Science and Technology, Pohang, 790-330, Korea  
and Basic Science Branch, Research Institute of Industrial Science and Technology, Pohang 790-330, Korea*

H. Kang

*Chemistry Department, Pohang Institute of Science and Technology, Pohang 790-330, Korea  
and Basic Science Branch, Research Institute of Industrial Science and Technology, Pohang 790-330, Korea*

J. W. Chung

*Physics Department, Pohang Institute of Science and Technology, Pohang, 790-330, Korea  
and Basic Science Branch, Research Institute of Industrial Science and Technology, Pohang 790-330, Korea*

(Received 29 April 1993; revised manuscript received 17 September 1993)

We report results of a combined study of *in situ* x-ray-photoemission spectroscopy (XPS) and low-energy-electron diffraction (LEED) for silicon nitride films fabricated at room temperature. A variety of nitride films of  $SiN_x$  ( $0.2 \leq x \leq 1.33$ ) were formed by bombarding low-energy nitrogen ions ( $E \leq 600$  eV) onto a Si(001) surface without thermal treatment. The results reveal that the Si-N bond nature in the ion-deposited layers (IDL's), derived from the characteristic XPS spectra, strongly resembles that of a typical thermally prepared silicon nitride,  $\beta$ - $Si_3N_4$ . We find the chemical shift per Si-N bond to be 0.62 eV, and a shift of Fermi level due to nitridation less than 0.1 eV. We estimate the thickness of the unannealed IDL's to be less than 18 Å. Upon annealing an IDL, progressive changes of XPS peaks and LEED patterns suggest that nitrogen atoms migrate from initial metastable defect sites to thermally stable sites, and tend to coalesce to form locally ordered microcrystallites. The thermal activation energy barrier in an IDL of  $E = 400$  eV,  $x = 1.33$  is found to be about 0.21 eV, in agreement with theoretical predictions.

**I. INTRODUCTION**

Silicon nitride films ( $\alpha$ - and  $\beta$ - $Si_3N_4$ ) have been widely used in silicon-based microelectronics devices as passivation layers, insulating barriers in thin-film transistors, and diffusion barriers in multilayer devices.<sup>1,2</sup> A number of methods to produce such nitride films have been developed over the past decades in order to improve the film quality by fine control of various defects in the films.<sup>1-5</sup> However, almost all the methods inevitably adopt high-temperature thermal annealing under ambient pressure of impurities, which results in the degradation of the physical properties of the films. Typical examples for such uncontrolled imperfections are hydrogen and oxygen impurities, and thermally induced defects such as vacancies and dislocations. Hydrogen impurities are known to affect sensitively the trap states and reduce the midgap density of states (DOS).<sup>3</sup> Therefore characterization of nitride films has usually been complicated by such uncontrolled defects incorporated during fabrication procedures.

Among the two isomorphs of silicon nitrides,  $\alpha$ - and  $\beta$ - $Si_3N_4$ , the Si-N chemical bond structure in the  $\beta$  phase, which is not complicated by impurities, has been well described in terms of a continuous random network of  $SiN_4$  tetrahedra.<sup>3,4</sup> In this model, silicon atoms have four neighboring nitrogen atoms, while each nitrogen atom locates at a planar, triply coordinated site with three nearest silicon neighbors.<sup>4,5</sup> This model accounts reasonably well for the results from experiments including x-ray<sup>6</sup> and inelastic neutron diffraction,<sup>7</sup> electron-energy-loss spectroscopy (EELS),<sup>8</sup> and photoemission spectroscopy.<sup>3,4</sup>

In this paper, we describe several important physical

properties, including progressive changes of the local Si-N bond structure, atomic positional order, and thermal behavior of ion-deposited nitride layers (IDL's),  $SiN_x$ , as a function of nitrogen content  $x$ . The method, which has been applied previously to form a thin nitride film,<sup>9</sup> utilizes a beam of low-energy ( $\leq 600$  eV)  $N_2^+$  ions impinging on a Si(001) surface at room temperature under UHV environment. Detailed characteristics of the resulting films are analyzed in terms of a modified random network model. In this modified version, nitrogen atoms are allowed to occupy either the planar trigonal sites of  $sp^2$  or the pyramidal tetrahedral sites of  $sp^3$  bonding character. We discuss the physical properties of the films in comparison with those of a thermally prepared amorphous silicon nitride ( $\alpha$ - $Si_3N_4$ )<sup>3,9</sup> with an emphasis on several distinct differences.

**II. EXPERIMENT**

The experiments were carried out using an x-ray-photoemission spectroscopy (XPS) spectrometer and a high-resolution low-energy-electron-diffraction (LEED) system under a base pressure of  $5 \times 10^{-11}$  mbar. We utilized a Mg  $K\alpha$  ( $h\nu = 1253.6$  eV) radiation of linewidth about 0.73 eV for XPS measurements. The binding energy  $E_b$  was referenced to a Fermi level, which was calibrated by Au  $4p_{7/2}$  and Cu  $p_{3/2}$  peaks at  $E_b = 83.8$  and 932.5 eV, respectively. The high-resolution LEED system, which has been described elsewhere,<sup>10</sup> was used primarily to identify the degree of positional order on the sample surfaces, and has an effective transfer width of above 1000 Å. In order to quantify the high-resolution LEED patterns, a series of two-dimensional scans that show spot profiles was obtained.

Using a beam of low-energy ( $150 \leq E \leq 600$  eV)  $N_2^+$  ions striking a substrate surface at room temperature, we were able to fabricate a series of the IDL's,  $SiN_x$ , with a nitrogen content  $x$  in the range  $0.22 \leq x \leq 1.33$ . The total number of nitrogen ions to which a sample was exposed was controlled by varying exposure time and is expressed in the units of monolayers ( $1 \text{ ML} = 6.8 \times 10^{14}$  atoms/cm<sup>2</sup>). We determined  $x$  by measuring nitrogen-associated XPS peaks, Si 2p and N 1s normalized by Si 2p from a clean Si(001) surface. A beam of  $N_2^+$  ions was produced by the same way adopted in previous studies<sup>11,12</sup> by replacing oxygen gas with high-purity ( $\geq 5N$ ) nitrogen gas. The ion current decreased rapidly with decreasing ion energy  $E$  producing  $10^{-6}$ – $10^{-8}$  A when  $E$  varied from 600 to 150 eV. We did not attempt to fabricate an IDL with  $E < 150$  eV because of significantly reduced ion current.

The substrate was a boron-doped silicon (001) crystal with a resistivity of 4–6  $\Omega$  cm and dimensions of  $5 \times 25 \times 1$  mm<sup>3</sup>. Repeated heating of the sample up to 1250°C followed by a brief annealing at 600°C normally produced a clean reconstructed surface showing a sharp ( $2 \times 1$ ) LEED pattern. We heated the sample resistively by passing ac current directly through the sample, and measured sample temperatures using an optical pyrometer, while recording the current at the same time. A set of measured data of temperature versus current produced an empirical formula, which was used to convert currents to temperatures for the XPS spectra. This made data acquisition of XPS spectra as a function of temperature relatively easy.

### III. RESULTS AND DISCUSSION

#### A. Fabrication of a $SiN_x$

A plot of nitrogen content  $x$  in a  $SiN_x$  layer as a function of  $N_2^+$  ion exposure at room temperature is shown in Fig. 1 for various ion energies. We observe two stages of nitrogen uptake, i.e., initially  $x$  rises rapidly in propor-

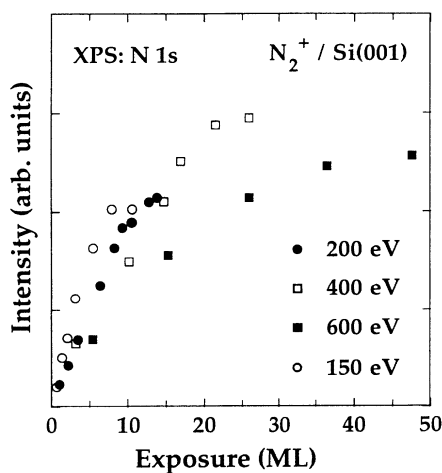


FIG. 1. Nitrogen content  $x$  determined from the N 1s XPS peak intensity in the IDL's of various ion energies. It is apparent that lower-energy ions are more effective to form an IDL for a given exposure. However, the maximum nitrogen content increases with ion energy due to the deeper nitrided layer.

tion to the ion exposure and then reaches a plateau. The slope at the initial stage of nitrogen uptake apparently increases with decreasing ion energy, which implies that the lower-energy ions are more effective to form a  $SiN_x$  layer. We also note that the plateau increases with ion energy except for the case of ions with  $E = 600$  eV. The increase of maximum nitrogen content was also observed for IDL's with  $E \leq 200$  eV,<sup>4</sup> and oxygen-ion-deposited  $SiO_2$  layers.<sup>11,12</sup> As pointed out in the previous work,<sup>11</sup> the lower plateau for  $SiN_x$  of  $E = 600$  eV ions is caused by more significant self-sputtering effect compared to deposition.

In order to estimate the thickness  $t$  of an IDL, we measured a Si 2p peak intensity  $I_1$  from an IDL, which is normalized by the intensity  $I_2$  from a clean silicon substrate. We may estimate a thickness from an expression,<sup>13</sup>

$$\frac{I_1}{I_2} = \frac{d_1 \lambda_1}{d_2 \lambda_2} (e^{t/\lambda_1} - 1), \quad (1)$$

where  $d_1, d_2$ , and  $\lambda_1, \lambda_2$  denote densities and electron mean free paths in an IDL, and in a pure silicon substrate, respectively. Using  $d_1/d_2 = 0.823$ ,<sup>14</sup> and  $\lambda_1 = 36$  Å,  $\lambda_2 = 27$  Å for Mg  $K\alpha_1$  x ray (1253.6 eV),<sup>15</sup> we obtained 13, 17, and 16 Å for annealed IDL's of  $x = 1.33$  formed by ions of  $E = 200, 400$ , and 600 eV, respectively. These values for thickness of the IDL's are comparable with 19 Å obtained for an IDL of  $E = 500$  eV by Taylor *et al.*<sup>15</sup>

#### B. XPS core-level spectra of the IDL's

A set of Si 2p core-level spectra from the IDL's of  $E = 400$  eV as a function of nitrogen content  $x$  are shown in Fig. 2. We stress that our Si 2p spectra are significantly different from those of Karcher, Ley, and Johnson<sup>3</sup> in that the Si 2p peak consists of two separated peaks for IDL's rather than a single broadened one for an  $a$ - $SiN_x$ . The different line shapes are partially ascribed to

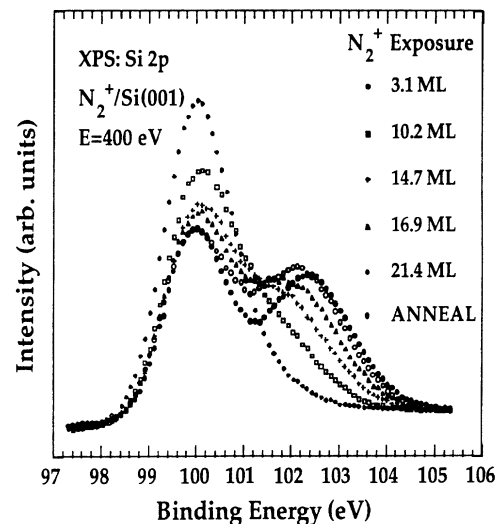


FIG. 2. A progressive change of Si 2p XPS spectra from an IDL of  $E = 400$  eV with  $N_2^+$  ion exposure in the units of monolayer ( $1 \text{ ML} = 6.8 \times 10^{14}$  atoms/cm<sup>2</sup>). Notice that intensity of the peak near 100 eV decreases while another peak near 102.5 eV concomitantly grows with ion exposure.

the way the nitrides were formed, i.e., in our work, the nitride films are relatively thin and are formed only near the surface region. Therefore our XPS spectra essentially contain significant contributions from underlying substrate silicon atoms. On the other hand, Karcher, Ley, and Johnson used  $\alpha$ -SiN<sub>x</sub> where nitrogens are distributed uniformly throughout the sample. It is worthwhile to note that the satellite peak near  $E_b = 102$  eV is close to that of the  $\beta$  isomorph of thermal silicon nitrides.<sup>3</sup> The fact that the satellite peak near  $E_b = 102$  eV in Fig. 2 grows rather rapidly with  $x$  implies that the local Si-N bond structure may be similar to that of a  $\beta$ -Si<sub>3</sub>N<sub>4</sub>, even at very early stage of nitridation.

In order to analyze the Si 2*p* XPS spectra quantitatively, we adopted a model that accounts well for the chemical bond configurations in thermal silicon nitrides.<sup>3</sup> The model proposes that a Si 2*p* peak consists of five components, Si<sup>(*n*)</sup> ( $n=0,1,2,3,4$ ), denoting a silicon atom with  $n$  nitrogen neighbors. Assuming that each component has a line shape identical to that of a pure silicon, Si<sup>(0)</sup>, and its binding energy is equally spaced, we deconvoluted the spectra as illustrated in Fig. 3. Such a deconvolution allows us another independent way to estimate nitrogen content  $x$  and the chemical shift of Si 2*p*,  $\Delta E_b(\text{Si } 2p) = E_b(\text{Si}^{(4)}) - E_b(\text{Si}^{(0)})$ . We obtain  $\Delta E_b(\text{Si } 2p) = 2.48$  eV for the annealed IDL of  $x = 1.33$  in Fig. 2, corresponding to 0.62 eV per Si-N bond, in close agreement with previous study for thermal silicon nitrides.<sup>3,9,16</sup>

It is interesting to note that the Si<sup>(0)</sup> component in the annealed IDL has no significant shift [ $\Delta E_b(\text{Si}^{(0)}) \leq 0.1$  eV] as  $x$  varies from 0.22 to 1.33, in sharp contrast to that of a thermally prepared silicon nitride, which shows  $\Delta E_b(\text{Si}^{(0)}) = 0.6$  eV.<sup>3</sup> However, we observe  $\Delta E_b(\text{N } 1s) = +0.7$  eV for the same range of  $x$ , similar to a thermal nitride. Karcher, Ley, and Johnson<sup>3</sup> attributed this shift of +0.6 eV for both Si 2*p* and N 1*s* peaks to the shift of Fermi level  $E_F$ . Our results, however, suggest that the Fermi level

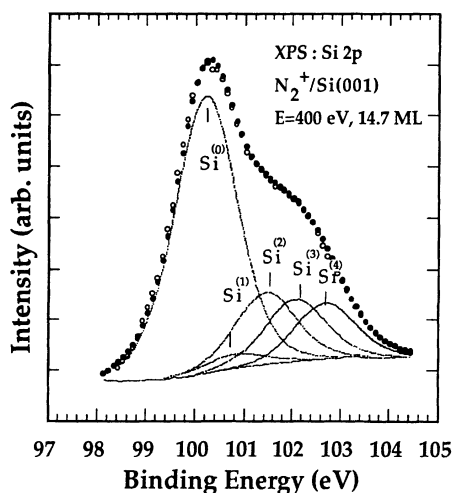


FIG. 3. A typical spectrum fitted by five curves representing five different Si-Si<sub>4-n</sub>-N<sub>4</sub> bond configurations in the IDL of  $E = 400$  eV, ion exposure of 14.7 ML. Open and solid circles denote experimental and fitted data, respectively. The inner five curves show intensities and positions of five components Si<sup>(*n*)</sup> ( $n=0,1,2,3,4$ ).

shift is at most 0.1 eV and  $\Delta E_b(\text{N } 1s) = +0.7$  eV is mostly a chemical shift caused by the change of charge distribution near N atoms as bond configuration changes with  $x$ .

In Fig. 4, we show the relative abundance of each component, represented by its intensity  $I(\text{Si}^{(n)})$ , as a function of  $x$ . We observe that the Si<sup>(4)</sup> component, which is a regular bond structure of a  $\beta$ -Si<sub>3</sub>N<sub>4</sub>, increases rapidly as  $x$  increases while Si<sup>(0)</sup> decreases concomitantly. Also note that for  $x \geq 0.5$ , Si<sup>(1)</sup> almost vanishes, indicating that there is no isolated single Si-N bond unit. We thus confirm that N 2*p* electrons always couple with at least two or more Si 3*p* and 3*s* electrons as suggested earlier.<sup>3-5</sup> For  $x$  near 1.33, the stoichiometric value of a  $\beta$ -Si<sub>3</sub>N<sub>4</sub>, the main component of bond configurations is Si<sup>(4)</sup>, close to that of a thermal  $\alpha$ -Si<sub>3</sub>N<sub>4</sub>.

As was done in previous work,<sup>3</sup> we can also evaluate the nitrogen content  $x$  from the results of above fits using a weighted average of the intensities of each component [see Eq. (1) in Ref. 3]. The results thus obtained from Si 2*p* spectra,  $x(\text{Si } 2p)$ , are compared with those from N 1*s* spectra,  $x(\text{N } 1s)$ , in Fig. 5 for IDL's of  $E = 400$  (open circles) and 600 eV (solid circles). We observe that the least-squares fits (solid lines) for both sets of data produce straight lines. The lines have slopes quite close to unity, indicating that almost all the deposited nitrogen ions form Si-N bonds, thus leaving not many wrong bonds of N-N type, especially at high  $x$ , in contrast to the thermal nitrides, where the data deviate from the linear behavior.<sup>3</sup>

However, the fact that  $x(\text{Si } 2p)$  underestimates the nitrogen content in comparison with  $x(\text{N } 1s)$ , as seen in Fig. 5 by the small offsets from the origin for both lines, implies a possibility of the presence of undercoordinated Si-N bonding units. This becomes more apparent when we evaluate the coordination number at a N site, defined as  $C \equiv 3x(\text{Si } 2p)/x(\text{N } 1s)$ , which is less than 3 for all  $x$  (see the inset in Fig. 5). Since  $C = 3$  for an ideal  $\beta$ -Si<sub>3</sub>N<sub>4</sub>, we find that the IDL's have a few percent, ranging from 3 to

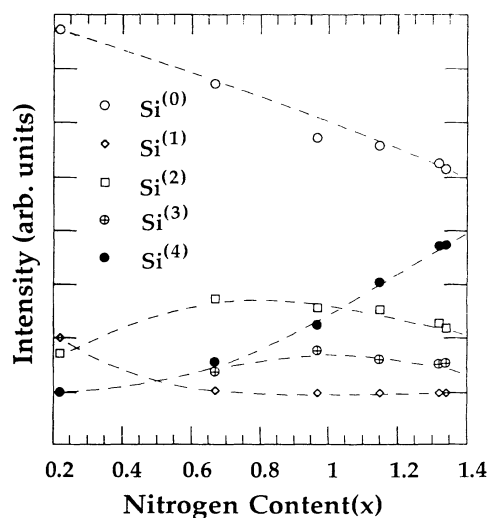


FIG. 4. Relative abundance of five components Si<sup>(*n*)</sup> vs nitrogen content  $x$  in the IDL's of  $E = 400$  eV. It is seen that Si<sup>(0)</sup> drops rapidly while Si<sup>(4)</sup> rises correspondingly with increasing  $x$ . The dotted curves are drawn to guide the eye.

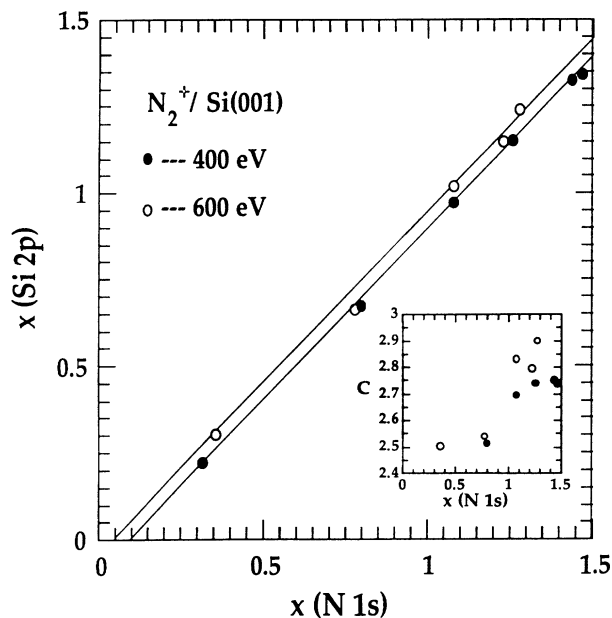


FIG. 5. Nitrogen content in the IDL's of  $E = 400$  eV (open circles) and  $600$  eV (solid circles) determined from the normalized intensities of the Si  $2p$  peak,  $x(\text{Si } 2p)$ , vs that from the N  $1s$  peak,  $x(\text{N } 1s)$ . Note that  $x(\text{Si } 2p)$  slightly underestimates in comparison with  $x(\text{N } 1s)$  as denoted by the two nearly parallel straight lines slightly off the origin. The inset shows that the coordination number  $C$  at a nitrogen site increases with  $x(\text{N } 1s)$ , reflecting the rise of  $\text{Si}^{(4)}$  component in Fig. 4.

16%, of undercoordinated Si-N bond population which varies with  $x$ . The coordination numbers estimated for the IDL's are similar to those deduced from x-ray- and neutron-diffraction measurements for high-temperature chemical-vapor-deposited (CVD) nitrides.<sup>3,6,7</sup>

### C. XPS valence-band spectra of the IDL's

A series of XPS valence-band spectra of IDL's for various  $x$  are shown in Fig. 6. The bottom spectrum from  $x = 0$  shows a typical XPS valence-band feature of a pure silicon substrate, which reveals two characteristic peaks with their spectral weights centered near  $E_b = 4.4$  and  $10.0$  eV and another wide peak near  $23$  eV. The two peaks in the low-binding-energy side, and the broad one in the high-binding-energy side are basically from the Si  $3p$ , and  $3s$  states, and plasmons excited by the outgoing photoelectrons, respectively.<sup>3,4,17,18</sup>

We observe several characteristic features of these peaks with increasing  $x$ , as summarized as follows. (i) The peak at  $4.4$  eV shifts toward the high-binding-energy side at an early stage of  $x = 0.22$  by about  $+0.6$  eV and then remains almost unshifted up to  $x = 1.33$  (peak A). (ii) The peak at  $10.0$  eV develops rapidly into two peaks as soon as nitrogens are incorporated, one at a lower- (peak B) and another at the higher-binding-energy side (peak C). The two peaks continue to shift gradually with increasing  $x$  as depicted by the vertical lines. The features for  $E_b \leq 14$  eV ultimately form a characteristic A-B-C structure for IDL of  $x = 1.33$  with peaks at

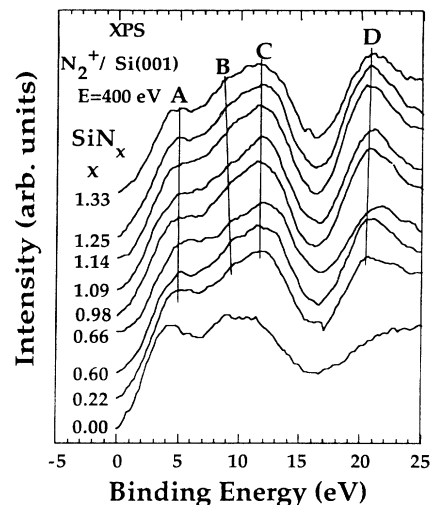


FIG. 6. A series of XPS valence spectra for various  $x$ . Three nearly vertical lines show gradual shifts of the characteristic A, B, and C peaks with  $x$ . Note that as early as  $x = 0.22$ , the A-B-C structure below  $E_b \leq 14$  eV is apparent. Also note that the broad plasmon peak near  $23$  eV becomes dominated by the strong N  $2p$  peak denoted as peak D.

$E_b = 5.0, 8.6,$  and  $11.7$  eV, similar to that of a  $\beta\text{-Si}_3\text{N}_4$ .<sup>3,4,18</sup> Isu and Fujiwara<sup>19</sup> observed a similar structure with peaks at  $E_b = 4.2, 7.2,$  and  $10$  eV on a nitrated Si(111) surface, while Karcher, Ley, and Johnson<sup>3</sup> reported peaks at  $E_b = 4.9, 7.9,$  and  $10.7$  eV on silicon nitrides produced by a dc-sputtering method. The  $E_b$ 's of the characteristic A, B, and C peaks estimated in this study are slightly different from those reported earlier due to different contributions from the sublayer silicon atoms.

We also note that a small DOS,  $0.5$  eV below  $E_F$  due to the surface states originated from the dangling bonds on the clean silicon surface, decreases rapidly with  $x$ , causing a shift of valence-band maximum (VBM) toward the high-binding-energy side and thus increasing the energy gap. However, due to the finite thickness ( $\leq 17$  Å) of the IDL's, which is shorter than the probing depth of photoelectrons ( $\sim 30$  Å), the recession of VBM is not as significant as in a bulk thermal  $\alpha\text{-Si}_3\text{N}_4$ .<sup>3,4</sup> The broad plasmons on the high-binding-energy side become dominated by a strong N  $2s$  electron (peak D in Fig. 6) for IDL's with  $x$  as low as  $0.22$ .

The close similarity of the valence-band spectra for  $x \geq 0.60$  with that of a thermally prepared  $\text{Si}_3\text{N}_4$  indicates that most nitrogens in the IDL's are located at the triply coordinated planar, or nearly planar pyramidal sites as in a  $\alpha\text{-Si}_3\text{N}_4$ .<sup>3-5</sup> This matches our observations from the Si  $2p$  core level spectra as discussed earlier. The peaks A, B, and C are believed to originate from hybridization of N  $2p$  electrons with Si  $3s$  and  $3p$  electrons, and are well reproduced in theoretical DOS of  $\beta\text{-Si}_3\text{N}_4$  by several authors.<sup>18,20</sup> It is interesting to note that the N  $2s$  state shows relatively small changes of  $E_b$  ( $\leq 2.0$  eV), in contrast to  $5.0$  eV reported for a thermal  $\alpha\text{-Si}_3\text{N}_4$  or a hydrogenated thermal  $\alpha\text{-Si}_3\text{N}_4$ .<sup>3</sup> We ascribe the difference also to the finite thickness of the IDL's. We thus find

that the IDL's produced by slow  $N_2^+$  ions ( $E \leq 600$  eV) at room temperature have their electronic nature quite similar to that of a thermal  $\alpha$ - $Si_3N_4$ .

#### D. Atomic positional order in the IDL's

We have investigated progressive changes of LEED patterns as a function of  $x$  in order to explore a possibility of any ordered phases in the IDL's. For this purpose, we have used nitrogen ions of  $E = 150$  eV since the  $(2 \times 1)$  LEED pattern disappears rather quickly for the IDL's of higher ion energies. The sharp half-order LEED spots from the reconstructed  $(2 \times 1)$ -Si(001) surface become broader and weaker with increasing  $x$ , and disappear completely near  $N_2^+$  ion exposure less than 1.0 ML. Near the saturation of  $x = 1.33$ , the whole LEED pattern disappears, and shows only an intense irregular background indicating the complete loss of long-range order. When the saturated surface was annealed at temperature  $T_a = 900^\circ\text{C}$  for about two minutes, weak satellite peaks appear in the vicinity of normal spots as shown in Fig. 7(a), where scans along the two perpendicular directions,

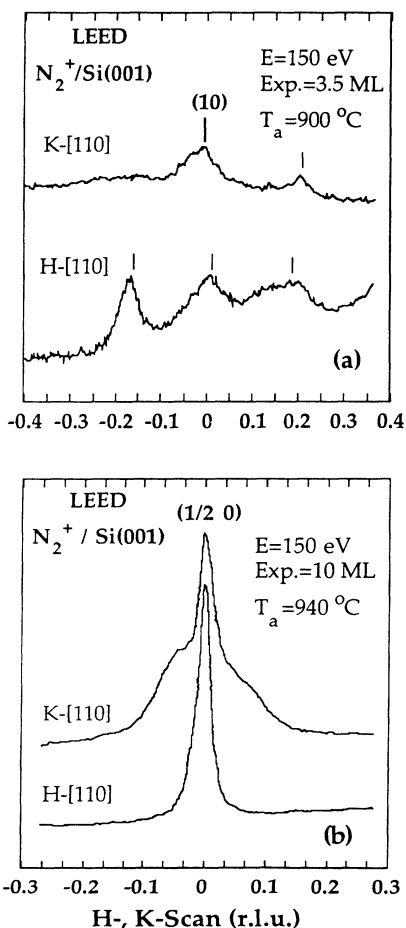


FIG. 7. Line scans along the  $H$  [110] and  $K$  [ $1\bar{1}0$ ] directions crossing (10) normal spot (a), and  $(\frac{1}{2} 0)$  superspot (b) of the  $(2 \times 1)$  phase of Si(001) surface. The IDL of  $E = 150$  eV, ion exposure of 3.5 ML (a) and 10 ML (b) was annealed at  $T_a = 900$  and  $940^\circ\text{C}$ , respectively, for about two minutes.

$H$ -[110] and  $K$ -[ $1\bar{1}0$ ] crossing the (10) spot, are presented. A two-dimensional scan shows a twofold symmetry for the whole LEED pattern. The scans in Fig. 7(a) were taken from an IDL with ion exposure of 3.5 ML.

The satellite peaks reveal that a certain degree of ordering has been developed in the IDL by thermal activation. Since the normal spots are still very weak, we infer that the order is very poorly developed at this stage, for example, in the form of a random distribution of small ordered domains, akin to the microcrystallites of  $\beta$ - $Si_3N_4$ . Similar trends have been observed from oxygen-ion-deposited  $SiO_2$  layers<sup>11,12</sup> and nitrogen-ion-deposited IDL's of  $E \leq 200$  eV formed on a Si(111) crystal,<sup>17</sup> where a comparatively well-developed LEED pattern, so-called quadruplet pattern, appears when annealed above  $950^\circ\text{C}$ .<sup>9,17,21,22</sup> We estimate the upper limit for the size of these microcrystallites in the IDL to be  $23 \text{ \AA}$  by measuring the full-width at half-maximum (FWHM) of the sharpest satellite peak.

The IDL in Fig. 7(a) was exposed further up to 10 ML and then annealed at  $T_a = 940^\circ\text{C}$  for an additional two minutes before taking similar scans crossing a half-order spot,  $(\frac{1}{2} 0)$ , as shown in Fig. 7(b). We observe asymmetric line broadening along the  $H$  and  $K$  directions, indicating a distribution of one-dimensional (1D) ordered domains in the IDL. Note that the broad tail along the  $K$  direction is a typical shape from a distribution of aggregates of locally ordered microcrystallites.<sup>11,23</sup> The ratio of FWHM's along the  $H$  and  $K$  directions suggests that the locally coherent region of a long rectangular shape silicon nitride domain is about one-seventh of the average domain size of the reconstructed  $(2 \times 1)$  phase. It is interesting to compare the 1D ordered nitride domain with the ordered line defects which consist of the dimer vacancies that are created by energetic  $Ar^+$  ions on the annealed Si(001) surface in a recent scanning-tunneling-microscope (STM) study by Feil *et al.*<sup>24</sup>

#### E. Thermal behavior of the IDL's

Since annealing of the IDL's generally produces better ordered nitride layers, we investigated thermal activation of nitrogen atoms in the IDL's in more detail as discussed below. Besides the changes of LEED patterns described in the preceding section, we also notice several important changes in the XPS spectra. As the annealing temperature  $T_a$  increases, the intensity of the N 1s peak decreases with a concomitant increase of Si 2p peak. The changes become more significant when annealed at about  $900^\circ\text{C}$ , for which the satellites as well as the half-order LEED spots of the  $(2 \times 1)$  phase reappear as mentioned before. Based on these observations, we propose a conceivable process that may be happening in the IDL's.

Nitrogen atoms in the room-temperature IDL's may initially occupy both stable and metastable sites, especially for those of undercoordinated bond configurations. When annealed, they can migrate by thermal excitation to more stable sites such as the triply coordinated sites in  $\beta$ - $Si_3N_4$ , and form aggregates of microcrystallites of  $\beta$ - $Si_3N_4$ , while leaving the remaining portion of the sample free of nitrogen atoms. This proposal explains reappear-

ance of the  $(2 \times 1)$  LEED spots together with the extra satellite spots from the annealed IDL. A small amount of nitrogen can also desorb or diffuse into the bulk deeper than the XPS probing length ( $\sim 30 \text{ \AA}$ ), and the newly exposed nitrogen-free silicon substrate should account for the changes of Si  $2p$  and N  $1s$  XPS peaks.

In order to evaluate a thermal activation-energy barrier in the IDL, we measured a series of Si  $2p$  spectra for various  $T_a$  and fitted the spectra as was done in Fig. 3. The results of the fits show a gradual increase of  $I(\text{Si}^{(0)})$  and  $I(\text{Si}^{(4)})$  that accompanies a decrease of other components with increasing  $T_a$ . This observation strongly supports our proposal that the initial bond structures in the IDL's are metastable, which can convert to the thermally stable structures by thermal diffusion over a potential barrier (activation energy  $E_d$ ) upon annealing. This thermally activated migration may be described in the framework of a thermal diffusion process. Since the thermal diffusion coefficient  $D$  shows an Arrhenius behavior,  $D = D_0 \exp(-E_d/kT)$ , and the total number of diffused particles for time  $t$  is proportional to  $(Dt)^{1/2}$ , the number of nitrogen atoms moved to thermally stable sites at temperature  $T$  is given by

$$n = n_0 e^{-E_d/2kT}, \quad (2)$$

where  $n_0$  is the number of nitrogen atoms initially located at metastable sites in an IDL. Since the intensity of an XPS peak is proportional to the number of atoms contributing to the peak, we plotted  $I(\text{Si}^{(4)})$  vs  $1/T$  in Fig. 8 for an IDL of  $E = 400 \text{ eV}$  and  $x = 1.25$ . The least-squares fit of the data in Fig. 8 produces  $E_d = 0.21 \text{ eV}$ , which is very close to a theoretical value of  $0.2 \text{ eV}$ . Hjalmarson, Jennison, and Binkley<sup>25</sup> predicted an activation energy barrier height of  $0.2 \text{ eV}$  between two possible binding sites of nitrogen in a silicon crystal, a metastable  $sp^3$  tetrahedral site and a stable off-centered  $sp^2$  planar trigonal state. It is also interesting to note that the activation energy of  $0.21 \text{ eV}$  is quite similar to that of  $0.22 \text{ eV}$  in a silicon dioxide film.<sup>12</sup>

In summary, we report that thin silicon nitride films

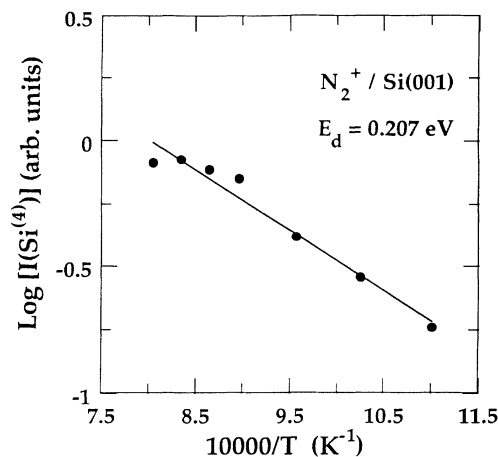


FIG. 8. Temperature dependence of the  $\text{Si}^{(4)}$  component in an IDL of  $E = 400 \text{ eV}$ ,  $x = 1.25$ . Least-squares fit of the data produces a thermal activation energy barrier of  $0.207 \text{ eV}$ , close to a theoretical value and that of an ion-deposited silicon oxide film.

are formed by bombarding low-energy nitrogen ions ( $E \leq 600 \text{ eV}$ ) on a Si(001) surface without thermal treatment. Bond configurations in the resulting films derived from characteristic XPS spectra are found to vary with nitrogen content  $x$  and become quite similar, albeit not identical, to those of a thermally prepared stable  $\beta\text{-Si}_3\text{N}_4$  at saturation of  $x = 1.33$ . The LEED investigation of the annealed IDL of  $x = 1.33$  suggests that the nitride layer may be composed of a number of small patches of ordered microcrystallites. We do not, however, exclude any inhomogeneous structures such as a percolating arrangement of  $\text{Si}_3\text{N}_4$ -like tetrahedra for the unannealed IDL's. We also find that formation of ordered microcrystallites upon annealing IDL of  $x = 1.33$  occurs through migration of nitrogen atoms from the metastable  $sp^3$  tetrahedral sites to the stable planar  $sp^2$  trigonal sites. Nitrogen atoms in the IDL's are found to occupy the defect sites, separated from the stable binding sites by an activation-energy barrier of  $0.21 \text{ eV}$ .

<sup>1</sup>M. J. Powell, B. C. Easton, and O. F. Hill, *Appl. Phys. Lett.* **38**, 794 (1981).

<sup>2</sup>For example, see John T. Milek, *Silicon Nitride for Microelectronic Application Part I. Preparation and Properties* (Plenum, New York, 1976); see also C.-E. Morosanu, *Thin Solid Films* **68**, 171 (1980).

<sup>3</sup>R. Karcher, L. Ley, and R. L. Johnson, *Phys. Rev. B* **30**, 1896 (1984).

<sup>4</sup>K. H. Park, B. C. Kim, and H. Kang, *J. Chem. Phys.* **97**, 2742 (1992).

<sup>5</sup>H. R. Phillip, *J. Electrochem. Soc.* **120**, 295 (1973); see also J. Robertson, *Philos. Mag.* **B 44**, 215 (1981).

<sup>6</sup>T. Aiyama, T. Fukunaga, K. Nihara, T. Hirai, and K. Suzuki, *J. Non-Cryst. Solids* **33**, 131 (1979).

<sup>7</sup>M. Misawa, T. Fukunaga, K. Nihara, T. Hirai, and K. Suzuki, *J. Non-Cryst. Solids* **34**, 313 (1979).

<sup>8</sup>D. H. Baek and J. W. Chung (unpublished).

<sup>9</sup>A. G. Schrott and S. C. Fain, Jr., *Surf. Sci.* **111**, 39 (1981); **123**, 204 (1982).

<sup>10</sup>D. H. Baek, J. W. Chung, and W. K. Han, *Phys. Rev. B* **47**, 8461 (1993).

<sup>11</sup>D. H. Baek, B. O. Kim, J. I. Jeong, C. Y. Kim, and J. W. Chung, *J. Appl. Phys.* **69**, 3354 (1991).

<sup>12</sup>J. W. Chung, D. H. Baek, B. O. Kim, H. W. Yeom, and C. Y. Kim, *Phys. Rev. B* **45**, 1705 (1992).

<sup>13</sup>T. A. Carlson and G. E. McGuire, *J. Electron Spectrosc. Relat. Phenom.* **1**, 5458 (1972/1973).

<sup>14</sup>D. Hardie and K. H. Jack, *Nature* **180**, 332 (1957).

<sup>15</sup>J. A. Taylor, G. M. Lanchester, A. Ignatiev, and J. W. Rabalais, *J. Chem. Phys.* **68**, 1776 (1978).

<sup>16</sup>G. M. Ingo, N. Zacchetti, D. Della ala, C. Coluzza, *J. Vac. Sci. Technol. A* **7**, 3048 (1989).

- <sup>17</sup>B. C. Kim, H. Kang, C. Y. Kim, and J. W. Chung (unpublished).
- <sup>18</sup>J. Robertson, *Philos. Mag. B* **63**, 47 (1991).
- <sup>19</sup>T. Isu and K. Fusiwara, *Solid State Commun.* **42**, 477 (1982).
- <sup>20</sup>S.-Y. Ren and W. Y. Ching, *Phys. Rev. B* **23**, 5458 (1981).
- <sup>21</sup>M. Nishijima, H. Kobayashi, K. Edamoto, and M. Onchi, *Surf. Sci.* **137**, 473 (1984).
- <sup>22</sup>R. Heckingbottom and P. R. Wood, *Surf. Sci.* **36**, 594 (1973).
- <sup>23</sup>M. Henzler, *Appl. Phys. A* **34**, 205 (1984).
- <sup>24</sup>H. Feil, H. J. W. Zandrliet, M.-M. Tsai, Jone D. Dow, and I. S. T. Tsong, *Phys. Rev. Lett.* **69**, 3076 (1992).
- <sup>25</sup>H. P. Hjalmarson, D. R. Jennison, and J. S. Binkley, in *Oxygen, Carbon, Hydrogen, and Nitrogen in Crystalline Silicon*, MRS Symposia Proceedings No. 59, edited by J. C. Mikkelsen, Jr., S. J. Pearton, J. W. Corbett, and S. J. Pennycock (Materials Research Society, Pittsburgh, 1986), p. 553.